



ORIGINAL ARTICLE

MONITOR CHANGES IN THE SPECTRAL INDICES VALUES OF SOIL SURFACE AND THEIR SPATIAL DISTRIBUTION USING REMOTE SENSING DATA

Mohammed A. Kadhim*, Salah M.S. Al-Atab and Jassim M. Saadoun

Department of Soil Science and Water Resources, College of Agriculture, University of Basrah, Iraq.

E-mail: muhamed.ahmed15@yahoo.com

Abstract: The study aims to monitoring the changes occurring in the values and area of the ground cover of the soil surface during the period 2006-2019 represented by water cover, wet areas, vegetation cover and soil erosion by applying mathematical relationships of a set of spectral indices specialized in studying soil and water. The spectral indices used in the study (EMI, NDWI, TCW and TCG). The results of the study showed a decrease in the values and area of the water cover represented by marshes, swamps and rivers due to the decrease in water levels and the increase in the phenomenon of drought in southern Iraq during the period 2006-2019, in addition to a great possibility to distinguish dry and barren lands from green lands, wet soils and droughts for agricultural uses. It can be concluded that the use of the TCG indices is important in diagnosing the vegetation cover in the study area, which was characterized by its content of plants, palm trees and vegetables, especially the banks of rivers and some reed and sedge plants in the marsh areas. Therefore, the study area was characterized by its low values and green areas and this is an indicator of the weak agricultural investment in it except for some regions. The results of the study also showed that there were levels of wind erosion during the period 2006-2019, ranging between very severe and low, the Dominance of very severe erosion throughout the study area, especially in the year 2006, where the area exposed to wind erosion amounted to about 4325.58 km², with a rate of 90.57%.

Key words: Spectral indices, Geographic information systems, Digital maps, Spatial variation.

Cite this article

Mohammed A. Kadhim, Salah M. S. Al-Atab and Jassim M. Saadoun (2020). Monitor Changes in the Spectral Indices Values of Soil Surface and their Spatial Distribution using Remote Sensing Data. *International Journal of Agricultural and Statistical Sciences*. DocID: <https://connectjournals.com/03899.2020.16.1981>

1. Introduction

Digital indices represent one of the most important improvements applied to satellite image, resulting from dividing the numerical values of one of the spectral bands by the corresponding values in another spectral band, and this is of great importance in transforming the spectral properties of the visual aspects affected by the luminosity, as these visuals show the variation in a curve Spectral reflectivity of the two respective bands regardless of the values of the reflectivity absorbed by the spectral bands [Hassan (2010)]. Digital indices are widely used in mineral investigation, plant analysis, desertification, and environmental monitoring, and is considered the best in distinguishing differences that

cannot be observed in satellite image with basic color bands, as well as reducing the effect of shadows in multi-spectral satellite image. There are many digital indices used in soil science studies. Fadhel (2009) found in his study the possibility of using the Tasseled Cap Transformation guide widely in agricultural and environmental studies in relation to the growth cycle of plants, soil properties and soil moisture, and it is one of the ways to improve the spectral information of satellite data by distinguishing dry lands from green lands and wet soils and determining the degrees of desertification and drought. As well as giving important information about soil and plants for agricultural uses. The study conducted by Al-Hayali (2017) showed the existence

of Spatial variance in the distribution of numerical indices values and their areas for the study area with significant relationships with NDWI index, SI index, NDSI index, TCW index and TCG index, and concluded that the spectral indices used in the study has a major role in distinguishing soil units, monitoring changes in vegetation cover, soil salinization, and distinguishing between wet and dry areas. Al-Saadi (2013) showed the possibility of using the Water Index (WI) to distinguish the state of water bodies on ground surfaces, as water has high spectral reflectivity within the visible light of the electromagnetic spectrum and low reflectivity to near infrared rays, so water appears in a dark color in the satellite image. He indicated that there is a sharp decline in the water areas represented by marshes, swamps, lakes and rivers due to the decrease in water levels and the prevalence of the phenomenon of drought in southern Iraq. He also used the Eolian Map Index (EMI) in his study and showed the importance of these indices in detecting areas exposed to wind erosion and containing sandy sediments on their surface. As it was able to find levels of wind erosion and dense sandy sedimentation within the southern desert region relatively large, followed by the eastern Shatt Al-Arab region, which reached high levels of wind erosion, while the marshes and tidal flats had lower values.

This study aimed to observe the changes occurring in the values and areas of the spectral indices of the soil surface and their spatial distribution by using the remote sensing data taken from the satellite image for different time periods to detect some of the changes occurring in the land cover and prepare digital maps for them.

2. Materials and Methods

2.1 Study area

The study area is located within the administrative boundaries of the province of Basra and Dhi Qar in Southern Iraq. It is part of the Iraqi alluvial plain and includes recently formed undeveloped soils with a limestone sedimentary origin within the order of Entisols. It is surrounded by streams of rivers and lakes of flood plains and has physiographic units representing the formations of the sedimentary plain, which consists of water deposits brought in by the Tigris and Euphrates and deposited in river floods as well as wind deposits transported by wind factors and dust storms. It is

bordered on the north by the confluence of the Tigris and Euphrates and Shatt Al-Arab rivers in the eastern part, and on the west by the dried up lands of the Hamar marsh. And located within the geographical location between latitudes 30° 27'24"-31°0'14" north and longitudes 46°30'56"-47°46'52" east and has an area of 4509.636 km² (Fig. 1).

2.2 The satellite images used in the study

The eight-band and the eleven-band satellite images were used for the Landsat 7 and Landsat 8 satellites and for the two sensors (OLI and ETM⁺) and captured during the periods 2006, 2014 and 2019 respectively. The satellite images were downloaded from the USGS site and its specifications are shown in Table 1. The study area was deducted using the computer program Arc map 10.4.1 to ensure a complete and accurate shape of the study area. The spectral contrast of the gray levels of the raw band visibility was converted into a chromatic composite visual using basic color compounds (RGB), and this method improves the visualization for distinguishing and identifying landmarks and ground coverings.

2.3 Remote sensing data

The aforementioned satellite images captured by the Landsat 7 and Landsat 8 satellites, respectively, were used and fully corrected. The satellite images were digitally processed using the Arc map 10.4.1 computer program. As the satellite images were used to extract the spectral data for the purpose of calculating the values of the digital indices used in the study, which are shown in Table 2.

2.4 Preparation of digital maps for spectral indices

Spectral indices were calculated using ArcMap10.4.1 for the years 2006, 2014 and 2019 respectively, after which their values were extracted and their areas were calculated in order to determine the changes that occurred in them during those years.

3. Results and Discussion

3.1 Spatial distribution of values and area (EMI)

Table 1: Satellite images used in the study.

The satellite	Resolution (m)	Sensor type	Date of capture
Landsat – 7	30	ETM ⁺	2006
Landsat – 8	30	OLI	2014
Landsat – 8	30	OLI	2019

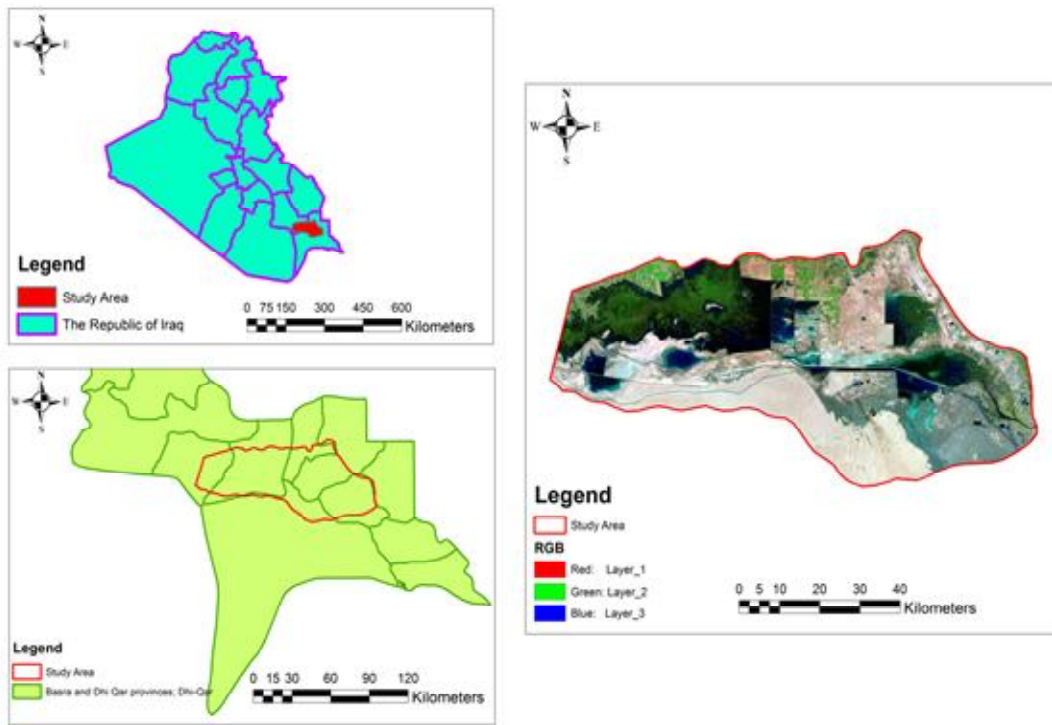


Fig. 1: Study area

Table 2: Spectral indices used in the study and their equations and references.

Indices	Full Name	Equation	References
EMI	Eolian map index	Red / NIR	(Kirey, 2007)
NDWI	Normalized Difference Water Index	$(Green - NIR) / (Green + NIR)$	(McFeeters, 1996)
TCW	Tasseled Cap Wetness	$= 0.1509*(B2)+0.1973*(B3)+0.3279*(B4) + 0.3406*(B5) - 0.7112*(B6) - 0.4572*(B7)$	(Fadhil, 2011)
TCG	Tasseled Cap Greenness	$= -0.2848*B2 - 0.2435*B3 - 0.5436*B4 + 0.7243*B5 + 0.0840*B6 - 0.180*B7$	(Crist and Kauth, 1986 ; Jensen, 1996)

Table 3: Spatial distribution of the EMI indices values classified according to area and percentage for the years 2006, 2014 and 2019

	VALUE	No. of Pixels	Pixel area	Percentage	Area Km2
Year 2006	(-11.30)-(1.21)	4806207	30 * 30	90.57	4325.58
	(1.22)-(13.40)	191949	30 * 30	7.91	172.75
	(13.41)-(16.50)	12606	30 * 30	1.52	11.34
Year 2014	(0.144)-(1.06)	957233	30 * 30	66.17	2980.75
	(1.07)-(1.71)	3311947	30 * 30	14.79	667.42
	(1.72)-(3.72)	741582	30 * 30	19.04	861.5
Year 2019	(0.132)-(1.27)	4327192	30 * 30	86.35	3894.47
	(1.28)-(2.26)	412939	30 * 30	8.25	371.64
	(2.27)-(8.90)	270631	30 * 30	5.4	243.56

in the study area

The results (Table 3 and Figs. 2, 3 and 4) showed a state of discrepancy in the values and area of the EMI index during the years 2006, 2014 and 2019 in the study area, as the index values ranged between (-11.30-

16.50), (-0.144-3.72) and (-0.132-8.90) respectively. As for its areas, it ranged between (11.34-4325.58), (667.42-2980.75) and (243.56-3894.47)km², respectively. The results showed the presence of levels of wind erosion in the study area during the period from

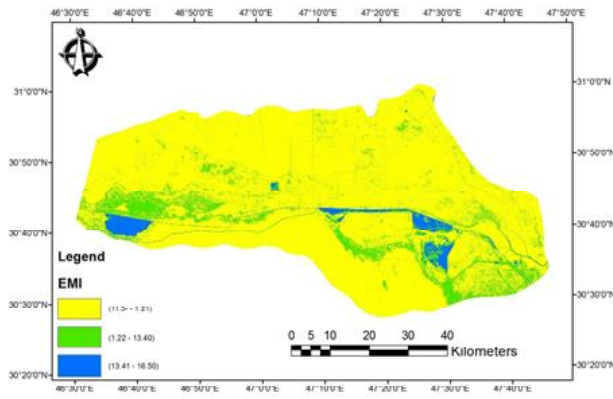


Fig. 2: Spatial distribution of the EMI index for the year 2006

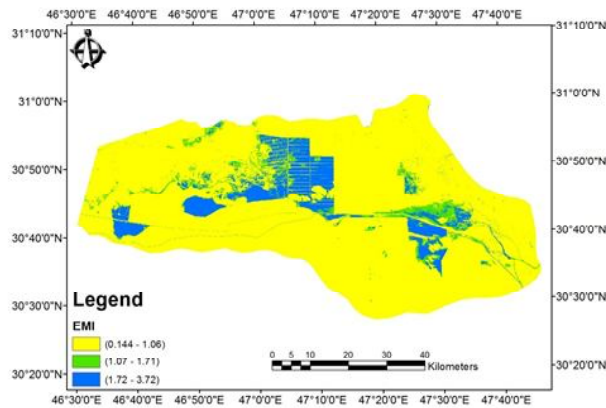


Fig. 3: Spatial distribution of the EMI index for the year 2014

2006 to 2019, as the yellow pixels represent areas of very severe erosion throughout the study area, especially in the year 2006, where the area exposed to wind erosion was about 4325.58 km², with a rate of 90.57%, followed by the green color pixels, which were areas of moderate wind erosion, especially in 2014, had an area of 667.42 km², with a rate of 14.79%. Whereas, the blue pixels are low-wind erosion marsh and rivers. The results indicate that the areas that were most exposed to wind erosion were in the year 2006 due to low precipitation rates, less vegetation cover and increased wind speed.

3.2 Spatial distribution of values and area (NDWI) in the study area

The results in Table 4 and Fig. 5, 6 and 7 showed a state of discrepancy in the values and area of the NDWI index during the years 2006, 2014 and 2019 in the study area, as the index values ranged between (− 0.767-1.08), (−0.759-0.673) and (−0.857-0.838) respectively. As for its areas, it ranged between (343.63-3158.09), (692.05-3018.29) and (485.16-3170.18) km²,

respectively. The results indicated that there are differences in the water index in the study area during the period from 2006 to 2019, and the dominance of the yellow and green pixels representing dry areas with little vegetation cover throughout the study area and for all the years were of negative values, while the blue pixels represented area of Marshes, swamps and rivers. The highest percentage of water index was in the year 2019, and it was 18.96%, with an area of 854.33 km², while the lowest percentage was in 2006, with an area of 343.63 km², with a rate of 7.62%. In general, it can be concluded that there is a decrease in the water areas represented by marshes, swamps, lakes and rivers due to the decrease in water levels as a result of natural and human conditions and thus the increase in the phenomenon of drought in southern Iraq during the period 2006-2019, and this corresponds to the study of Al-Saadi (012) on the phenomenon Desertification in southern Iraq.

3.3 Spatial distribution of values and area (TCW) in the study area

The results in Table 5 and Figs. 8, 9 and 10 indicated the existence of a discrepancy in the values and area of the TCW index during the years 2006, 2014 and 2019 in the study area, as the index values ranged between (−0.550-0.152), (−1.110-0.329) and (−1.310-0.670) respectively. As for its areas, it ranged between (428.86-2588.22), (713.58-2253.97) and (1169.04-

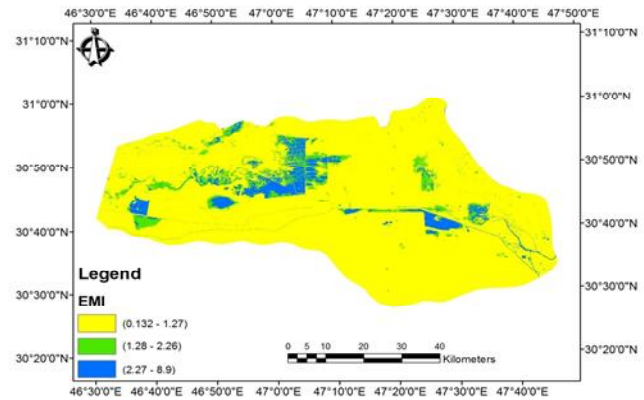


Fig. 4: Spatial distribution of the EMI index for the year 2019

1840.44) km², respectively. The results showed that there are variations in the TCW index in the study area during the period from 2006 to 2019, as the yellow pixels represented the barren areas throughout the study area, especially in the year 2006, with an area of 2588.22 km², with a rate of 57.39%, followed by the green pixels

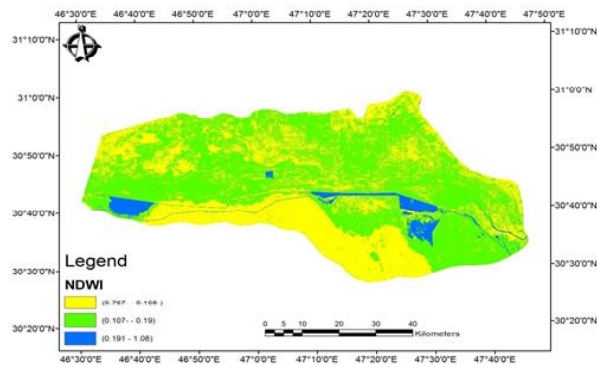


Fig. 5: Spatial distribution of the NDWI index for the year 2006

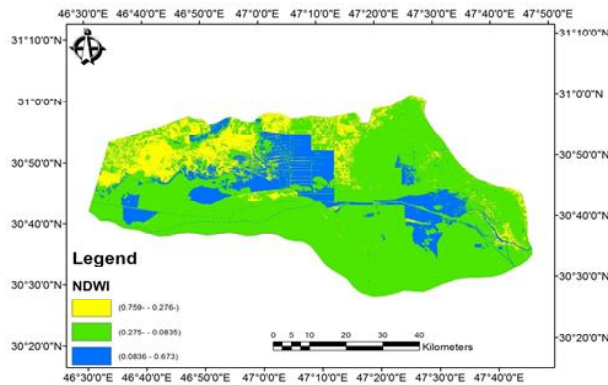


Fig. 6: Spatial distribution of the NDWI index for the year 2014

which are overlapping areas with the yellow-colored areas containing some natural plants with an area of 1492.59 km², with a rate of 33.09% for the same year, while the blue-colored pixels are wet areas with high water content, with an area of 1542.12 km², with a rate of 34.19%. As it was observed that there was an increase in the wet areas of the study area in terms of area and its percentage, which amounted to 34.19% and 33.27% for the years 2014 and 2019, respectively, as a result of the increase in precipitation rates during that period [Al-Hamdani (2017)]. Therefore, it can be concluded that the TCW index has great potential to distinguish dry and barren lands from green lands and wet soils and to determine the degrees of desertification and drought for agricultural uses, and it can be applied in agricultural and environmental studies for its close relationship with the plant growth cycle, soil characteristics and soil moisture.

3.4 Spatial distribution of values and area (TCG) in the study area

The results in Table 6 and Figs. 11, 12 and 13 showed a case of discrepancy in the values and area of the TCG index during the years 2006, 2014 and 2019

in the study area, as the index values ranged between (-0.138-0.167), (-0.203-0.720) and (-0.221-0.794) respectively. As for its areas, it ranged between (445.10-2588.22), (583.78-2884.32) and (406.86-3033.49) km², respectively. The results indicated that there were changes in the TCG index in the study area during the period from 2006 to 2019, as the blue pixels represented the vegetation areas and the cultivated areas throughout the study area and had an area of 583.78 km², with a rate of 12.94%, especially in the year 2014, while there was a decrease in their values. And its area in the rest of the years, followed by the yellow-colored pixels, which represented wet areas, lakes, swamps, and rivers, with less area than the green pixels that were represented by desert areas and devoid of water and green covers. Therefore, this index can be used in diagnosing the vegetation cover in the study area, which was characterized by its content of plants, palm trees and greenery, especially the banks of rivers and some reed and sedge plants in the marsh areas. The blue-colored pixels were distinguished from the rest of the regions by their low values and areas, and this is an indication of the weakness of agricultural investment in the study area, with the exception of some areas, and this corresponds to the study of Al-Jumaili (2012)

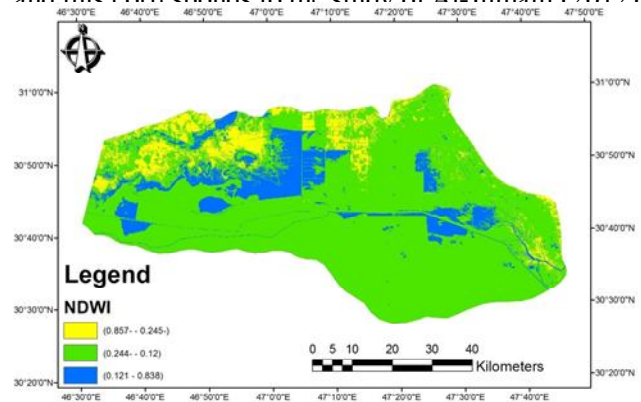


Fig. 7: Spatial distribution of the NDWI index for the year 2019

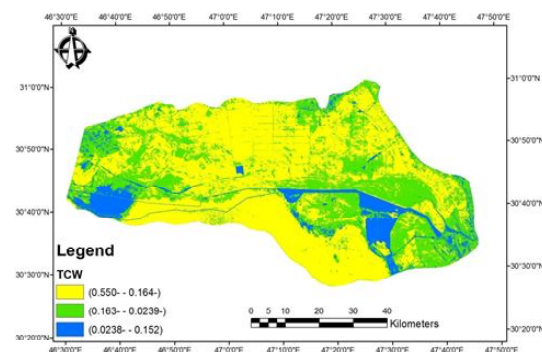


Fig. 8: Spatial distribution of the TCW index for the year 2006

Table 4: Spatial distribution of the NDWI indices values classified according to area and percentage for the years 2006, 2014 and 2019.

	VALUE	No. of Pixels	Pixel area	Percentage	Area Km2
Year 2006	(-0.767)-(-0.108)	1115383	30 * 30	22.26	1003.84
	(0.107)-(0.19)	3508998	30 * 30	70.03	3158.09
	(0.191)-(1.08)	381816	30 * 30	7.62	343.63
Year 2014	(-0.759)-(-0.276)	768950	30 * 30	15.36	692.05
	(-0.275)-(0.0835)	3353657	30 * 30	66.92	3018.29
	(0.0836)-(0.673)	888155	30 * 30	17.72	799.33
Year 2019	(-0.857)-(-0.245)	539069	30 * 30	10.75	485.16
	(-0.244)-(0.120)	3522431	30 * 30	70.29	3170.18
	(0.121)-(0.838)	949262	30 * 30	18.96	854.33

Table 5: Spatial distribution of the TCW indices values classified according to area and percentage for the years 2006, 2014 and 2019.

	VALUE	No. of Pixels	Pixel area	Percentage	Area Km2
Year 2006	(-0.550)-(-0.164)	2875809	30 * 30	57.39	2588.22
	(-0.163)-(-0.0239)	1658434	30 * 30	33.09	1492.59
	(-0.0238)-(0.152)	476519	30 * 30	9.52	428.86
Year 2014	(-1.110)-(-0.418)	2504415	30 * 30	49.98	2253.97
	(-0.417)-(-0.0447)	792875	30 * 30	15.83	713.58
	(-0.0446)-(0.329)	1713472	30 * 30	34.19	1542.12
Year 2019	(-1.310)-(-0.50)	2044942	30 * 30	40.81	1840.44
	(-0.449)-(-0.0507)	1298937	30 * 30	25.92	1169.04
	(-0.0506)-(0.670)	1666883	30 * 30	33.27	1500.19

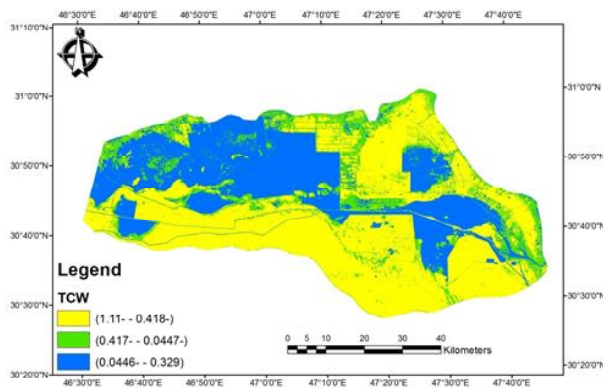


Fig. 9: Spatial distribution of the TCW index for the year 2014

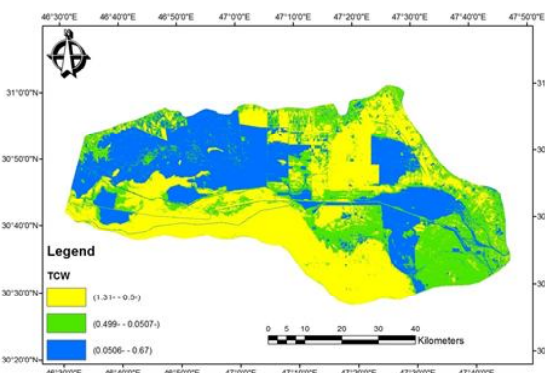


Fig. 10: Spatial distribution of the TCW index for the year 2019.

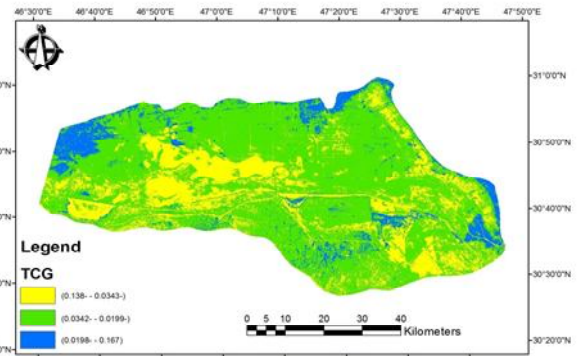


Fig. 11: Spatial distribution of the TGC index for the year 2006

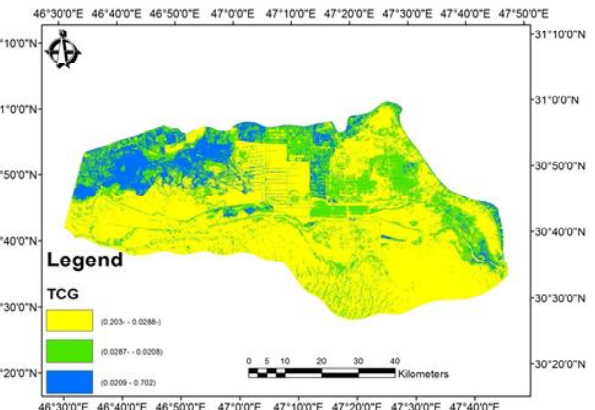
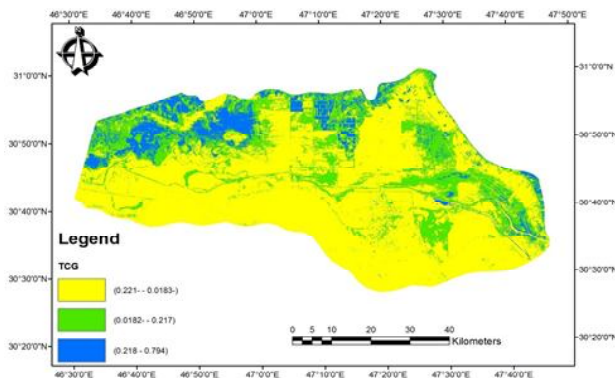


Fig. 12: Spatial distribution of the TGC index for the year 2014

Table 6: Spatial distribution of the TCG indices values classified according to area and percentage for the years 2006, 2014 and 2019

	VALUE	No. of Pixels	Pixel area	Percentage	Area Km2
Year 2006	(-0.138)-(-0.0343)	831276	30 * 30	16.59	748.14
	(-0.0342)-(-0.0199)	3684873	30 * 30	73.54	3316.38
	(-0.0198)-(0.167)	494557	30 * 30	9.87	445.10
Year 2014	(-0.203)-(-0.0288)	3204804	30 * 30	23.11	1041.58
	(-0.0287)-(-0.0208)	1157312	30 * 30	63.95	2884.32
	(0.0209)-(0.702)	648646	30 * 30	12.94	583.78
Year 2019	(-0.221)-(-0.0183)	3370549	30 * 30	23.71	1069.32
	(-0.0182)-(-0.217)	1188319	30 * 30	67.26	3033.49
	(0.218)-(0.794)	452074	30 * 30	9.03	406.86

**Fig. 13:** Spatial distribution of the TCG index for the year 2019

Acknowledgement

Authors thank the Editor and the referee for their insightful comments that led to substantive improvements of our article.

References

Al-Hamdany, A.S. (2017). Characterization, Classification and

Prediction of Soil Map Units by Using Remote Sensing and GIS in Bahar-Alnajaf, Iraq. *Ph.D Thesis*, College of Agriculture, University of Basra, Iraq.

Al-Hayali, M.A. (2017). Classification of some soils of eastern Shatt Al-Arab region in Basrah province and evaluation of land suitability for agricultural purposes by using remote sensing technologies. *Ph.D Thesis*, College of Agriculture, University of Basra, Iraq.

Al-Saady, A.K. (2013). A Studying of Land cover changes and Evaluation of Desertification State in the South of Iraq by Using Remote Sensing Techniques. *M.A. Thesis*, College of Science, University of Basra, Iraq.

Fadhel, A.M. (2009). Land degradation Detection Using Geo-Information Technology for some sites Iraq. *J. of AL-Nahrain Univ.*, **12(3)**, 94-108.

Hassan, A.A. (2010). A regional compositional study of the Al-Kaara region in the Iraqi Western Desert using satellite image. *M.A. Thesis*, College of Science, University of Baghdad, Iraq.